Numerical investigation of Australasian cold-formed steel strap-braced walls under lateral and vertical load

A. Karmakar, G.C. Clifton & J.BP.Lim

Department of Civil and Environmental Engineering, the University of Auckland, Auckland.

ABSTRACT

Cold-formed steel (CFS) has gained popularity in residential buildings due to its dimensional accuracy, lightweight, resistance to shrinking and creeping, durability, low embodied carbon and CNC manufacturing abilities. The steel used in CFS structures in New Zealand and Australia is higher strength and thinner gauge than those used in the Northern Hemisphere. Existing one and two-storey CFS buildings in New Zealand have shown excellent performance in severe earthquakes from 2010 to 2016. Several regions in New Zealand are now seeing an increased demand for medium-rise residential buildings up to around 6 storeys. Application of CFS into these buildings necessitates a different approach to that currently used in bracing and wall systems in two-storey buildings, which is the current limit on most CFS construction. The study investigates the behaviour of a proposed typical 0.95mm thick, grade 550 steel CFS strap-braced panel under lateral and vertical loading in the form of a seismic force-resisting system in SAP2000. The tension strap braces are yielded to accommodate seismic overloading and resist the failure of the connections, studs, chords or tracks using capacity-design principle. Various configurations of strap braces have been implemented and compared with the requirements of inter-storey drift of NZS 1170.5. The one-sided and both-sided strap-braced configurations resulted in the strength and stiffness requirements of the standard. A basis is formed for tension, compression and shear transfer mechanisms within the wall and from the wall to the foundation system. The horizontal and vertical stiffnesses of the wall/floor/wall connections on the wall's overall response are studied. The numerical analyses of the models show potential for such walls to be implemented in mid-rise buildings in New Zealand.

1 INTRODUCTION

The usage of cold-formed steel (CFS) has evolved over the years due to its innovation, which includes the advantages of high structural, technological and environmental performance (Macillo et al., 2014). Other characteristics like cost-effectiveness, light weight, resistance to insect attack, and easy and dry installation attracted the attention of industries across the world (Zeynalian & Ronagh, 2012), (Lee et al., 2014), (Pourabdollah et al., 2017), (Usefi et al., 2019). CFS has high dimensional accuracy and CNC manufacturing, making construction faster and easier. In addition, it also shows dimensional stability by resisting warping, shrinking and creeping under loads. These benefits, including low-cost maintenance and recycling capabilities, promote its usage development with the improvement of current design guidelines.

New Zealand is one of the major manufacturers of roll-forming machines, which are used to shape flat steel into the required profile shapes for CFS systems, and cold-formed steel-framed houses have existed for more than 50 years. Estimating material market share for residential construction is extremely difficult, and the majority of the time, the surveys tend to focus on traditional standalone houses built with traditional materials. The building consent without completion for multi-unit structures stands at 50%. Currently, the CFS industry takes up about 12% of the structural framing market. The properties of the steel used in New Zealand and Australia are high strength and thinner gauge steel, which is different to the steel used elsewhere worldwide. The minimum specified yield stress of CFS ranges up to 550 MPa, achieved due to work hardening during cold forming, and the thickness ranges from 0.42 mm to 1.5 mm. The ductility is limited, especially for steel thicknesses less than 0.9 mm (Hancock & Rogers, 1998).

When designing a cold-formed steel system, two commonly used terminologies are Lateral Force-Resisting System (LFRS) and Seismic Force-Resisting System (SFRS), which have a minor variation in their representation. According to the AISI Standard for Seismic Design of Cold-Formed Steel Structural Systems (AISI S400, 2020), the LFRS is the structural elements and connections that resist the racking and overturning due to the lateral forces, whereas the SFRS is the part of the structural systems that provides energy dissipation and resistance to the seismic forces. One commonly known SFRS incorporated using CFS is strap-braced walls, where energy dissipation occurs through the yielding of the tension strap braces (Madsen et al., 2016). Due to the capability to resist high lateral loads, CFS structures have gained popularity in low to mid-rise residential buildings in the northern hemisphere (Al-Kharat & Rogers, 2007), (Iuorio et al., 2014), (Gerami & Lotfi, 2014). Over the years, researchers termed resisting high seismic forces a significant advantage of CFS (Schafer et al., 2016), (Kasaeian et al., 2020). Many studies have shown that the strap braces connected to the chord-track joint through gusset plates bear good lateral stiffness and ductile behaviour (Hatami et al., 2008), (Davani et al., 2016), (Fiorino et al., 2016).

The traditional applications of CFS in New Zealand have been in one and two-storey houses, which showed excellent performance in recent severe earthquakes from 2010 to 2016. For mid-rise buildings, up to 6 storeys under the application of seismic loads necessitate a different approach than two-storey buildings. Diagonal strap braces act as tension members, which are connected to the chord track joint through gusset plates. These lateral load-resisting walls also act as vertical load-bearing walls for such structures. Lower-level mid-rise buildings are required to resist significant vertical loading during an earthquake and are subjected to combined lateral and vertical load. Extensive numerical modelling and experimental testing has been undertaken on CFS strap-braced walls under lateral loading in the northern hemisphere. However, there has been limited lateral load testing of the Australasian CFS strap-braced walls under the combination of lateral and vertical loading. The first tests under lateral and vertical loading were completed at the end of 2022 for a PhD project undertaken at the Structures Testing Lab of the University of Auckland.

The present numerical study investigates the behaviour of a proposed typical CFS strap-braced panel constructed from 0.95mm thick, grade 550 steel members under lateral and vertical loading using SAP2000 (Computer & Structures, 2022). The CFS walls are designed using capacity design principles to accommodate seismic overloading by yielding the strap braces in tension without failure of the connections, studs, chords or tracks. Different configurations of strap braces have been implemented to determine the inter-storey drift and compare that with the requirements of the Seismic Loadings Standard, NZS 1170.5 (Standards New Zealand., 2004). The analysis showed that one-sided and both-sided strap-braced configurations met the standard's strength and stiffness requirements. These numerical models have enabled an understanding of the tension, compression and shear transfer mechanisms within the wall panel and from the wall to the foundation system, which is required to achieve good wall/floor/wall performance when these walls form vertically stacked shear walls in mid-rise buildings. A stiff load path is required in the horizontal plane between adjacent vertical walls and between the bottom wall and the foundation, which prevents the failure of the wall tracks, which are weaker than the chords and studs. A range of realistic horizontal and vertical stiffnesses of the wall/floor/wall connections have been developed. The different analyses of the presented numerical models show potential for such walls to be implemented in mid-rise buildings in New Zealand.

2 ASSEMBLY OF THE CFS WALLS

SAP2000 is a general-purpose structural analysis and design program broadly used by industry engineers, but it has minimal capabilities to carry out finite element analysis. Therefore, the final boundary conditions of the presented CFS strap-braced walls were obtained through various assessments of the connections, which were updated throughout the modelling until the most realistic results were obtained. The systematic process of all the configurations is presented in the thesis (Karmakar, 2022).

2.1 Material properties

For the present numerical investigation, five numerical models have been developed to observe the lateral performance of the CFS strap-braced walls with a constant vertical load in SAP2000. The CFS walls are full-scale 2400 mm × 2400 mm specimens with the materials conforming to AS 1397-2021 (Standards Australia, 2021) and AS/NZS 4600:2018 (AS/NZS 4600, 2018). The thickness of the members is 0.95mm, and the grade is G500. The chords are back-to-back C sections placed 2400 mm apart, the dimensions between the C section studs are 600 mm, and the C section nogs are placed at equal distances from the bottom and top tracks. The chords are back-to-back lipped C sections with a depth of 89 mm and half top flange width of 40 mm, whereas the studs and nogs have a lip depth of 10 mm, flange width of 40 mm and depth of 89 mm. The gusset plates have a dimension of 300 mm × 300 mm with a thickness of 0.95 mm. The conventional configuration used for the numerical models and the cross-sectional view of the CFS members is shown in Figure 1. The web and the lips of the C section nogs are removed locally to allow for the passage of the studs. The adopted engineering values of yield stress, f_y, ultimate stress, f_u, and modulus of elasticity, *E*, of the CFS members are 500 MPa, 520 MPa and 205 MPa, respectively. The grade of the strap braces is adopted as G250 and the dimension is 80 mm in width and 0.95 mm in thickness. The yield stress, f_y, ultimate stress, f_u, and the modulus of elasticity, *E*, of the strap braces are 250 MPa, 320 MPa and 205 MPa, respectively.

2.2 Properties of the numerical models

The models have been developed to observe the overall system's lateral response, including the inelastic response of the strap braces beyond the yield point. The wall panels are also analysed to observe the influence of different levels of axial loads on the studs in conjunction with lateral loads. *Frame releases* with *partial fixity springs* are assigned to the frame members to represent the pinned connection between them. The chords are defined with rotational restraints about Y-axis with 10 kNm/rad springs, whereas the studs are rotationally restrained about the Y-axis with 1 kNm/rad springs. The connection between the nog flanges and stud flanges is effectively pinned in nature. Therefore, the nogs are rotationally restrained about the same axis with a 1 kN/mm partial spring. In practice, the pinned connection between the stud flanges and nog flanges can take a little compressive force and higher tension force. Since the cut-out is comparatively small, the nog provides resistance after a certain amount of movement when the stud tries to twist or move sideways. The strap braces are assigned to the wall panel with the pinned connection. The end releases are in the Y and Z direction for rotation and torsion at the initial end. The top and bottom tracks are modelled without any moment or shear releases to enable a stable response, as shown in Figure 1(a). The joint restraints assigned to each connection of the CFS walls are shown in Figure 1(b). The joints resulting from the bottom track and chords are pinned in connection, and therefore, the chord-bottom track joints are restrained for translation in the X and Y direction. The connection is also restrained for translation in the Z direction since the strap braces would develop an axial force in the bottom plate to the point of shear transfer to the foundation. At the same time, the chord-top track joints and studs-top track joints are restrained only in Y translation and are free to move in X and Z directions. The studs-bottom track joints are fixed in Y and Z translation and are free to move in the X direction.

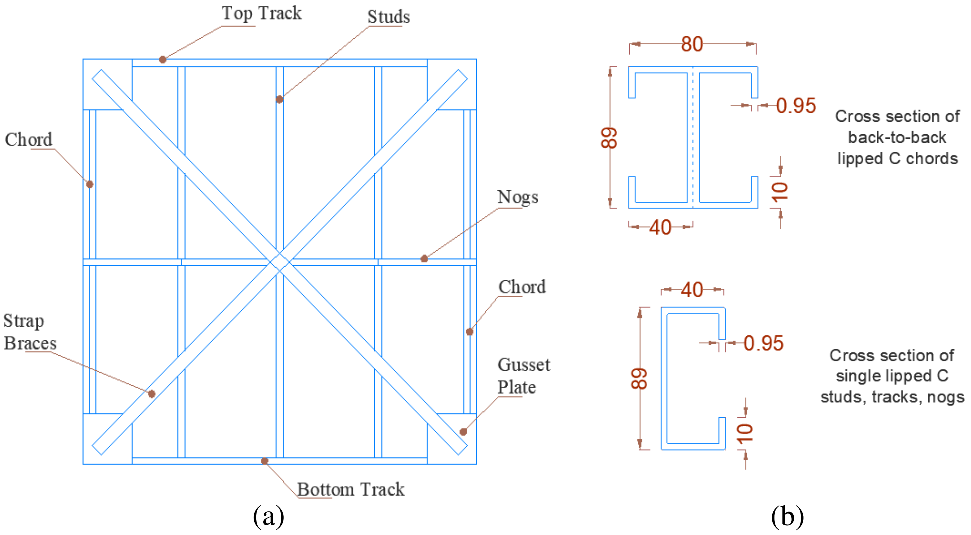

Figure 1 (a) A 2D illustration of the CFS strap-braced models and (b) a cross-section of the CFS members

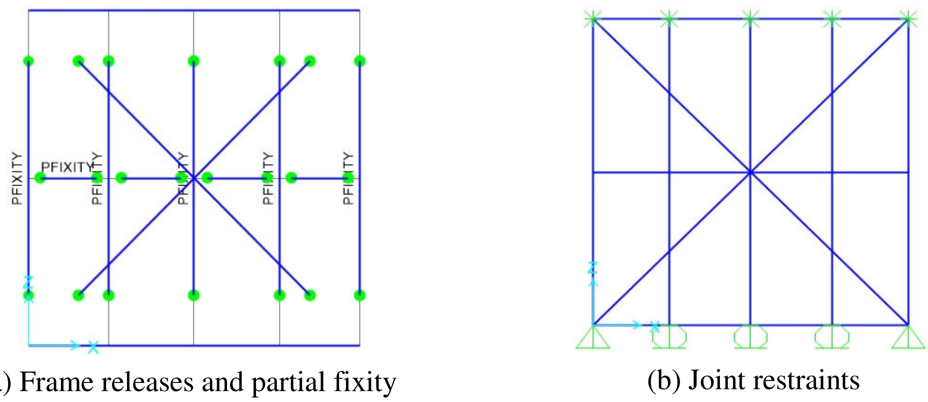

Figure 2 Frame and joint properties assigned to the CFS strap-braced wall panels

The strap braces act in tension as the SFRS members, dissipating energy through yielding. Utilising the X configuration braces through the capacity-based design generates resistance in both directions of lateral loading in the plane of the wall, with capacity design being used to prevent failure in the strap-to-gusset plate connections, chords and tracks. The energy dissipation of the CFS strap braces is obtained through the plastification and its connection to the other structural elements. *Compression limits*, a nonlinear property in SAP2000, are assigned for the strap braces to act as tension members. The strap braces are added to the wall system at an offset distance from the centre line of the CFS members to the centre line of the strap braces in the Y-axis on both sides of the panel. The ends are connected to the chord-track joint through *linear two-*

joint links with six degrees of freedom. The connection is made through the centroid of the strap braces to the centroid of the back-to-back channel section representing the connectivity of the nonlinear screws, as shown in Figure 2(a). *Thick shell elements* are used to model the gusset plates, which are connected to the chord-track joint, similar to the connection of the strap braces. A serial number of nodes are created in the centre line of the CFS frame elements and the shell element. These nodes are joined together using the two joint links. The grid lines in the Y axis are created and are joined through these nodes with each other using the two joint links, as shown in Figure 2(b).

The centreline distance between the strap braces and gusset plates is 0.95 mm. The default Auto Merge Tolerance in SAP2000 for basic tolerance check is 1 mm in metric units, and therefore, while modelling the strap braces lying on the gusset plates, by default, it is merged since the distance of the centre line of both elements is 0.95 mm. The simulation results in the interpretation that the strap braces' fibres are on the gusset plates' fibres and that they behave together.

In the numerical models, the tracks are constrained against sliding on their supports so that the horizontal component of strap tensile force can be distributed through the gusset plate into the track without causing any local track failure. In practice, the track is weaker than the chords and will fail unless the wall/floor/wall junction is sufficiently horizontally stiff to distribute this horizontal force between the tracks of adjacent walls or into the foundation at the base. That is the focus of the current phase of the research, through both experimental and numerical modelling and is beyond the scope of this paper.

2.3 Development of the numerical test models

Five numerical models are developed to observe the lateral performance with a constant vertical load which are described in Table 1. The *Model A* is built to observe the performance of the wall without any lateral bracing system, and hence no strap braces are considered. The system will exhibit the response of the vertical load on the wall to enable comparison with the behaviour of the CFS walls under lateral loading and combined vertical and lateral loading. *Model B* is developed to observe the performance under lateral loads with one-side braces only. The model will be a useful system to illustrate the differences in the resistance and stiffness resulting due to asymmetricity of the strap braces. *Model C* is developed similarly to *Model B*, but instead, the strap braces are assigned to the wall panel on both sides. In this model, the energy dissipation of both-side strap braces would determine the system's strength, stiffness, and ductility under lateral loading.

In *Model D*, the strap braces are connected to the chords on one side of the wall through gusset plates. The model is developed to observe the stiffness and resistance provided by the gusset plate to the system under lateral loads but would specifically observe the differences in the resistance and stiffness resulting from the asymmetricity of the strap braces and gusset plates. *Model E* is similar to *Model C*, but instead, the strap braces are assigned to the wall panel on both sides through the connection of gusset plates. In this model, the energy dissipation of both-side strap braces would determine the system's strength, stiffness, and ductility under lateral loading. On the other hand, the gusset plates are expected to increase the strength and ductility of the overall system.

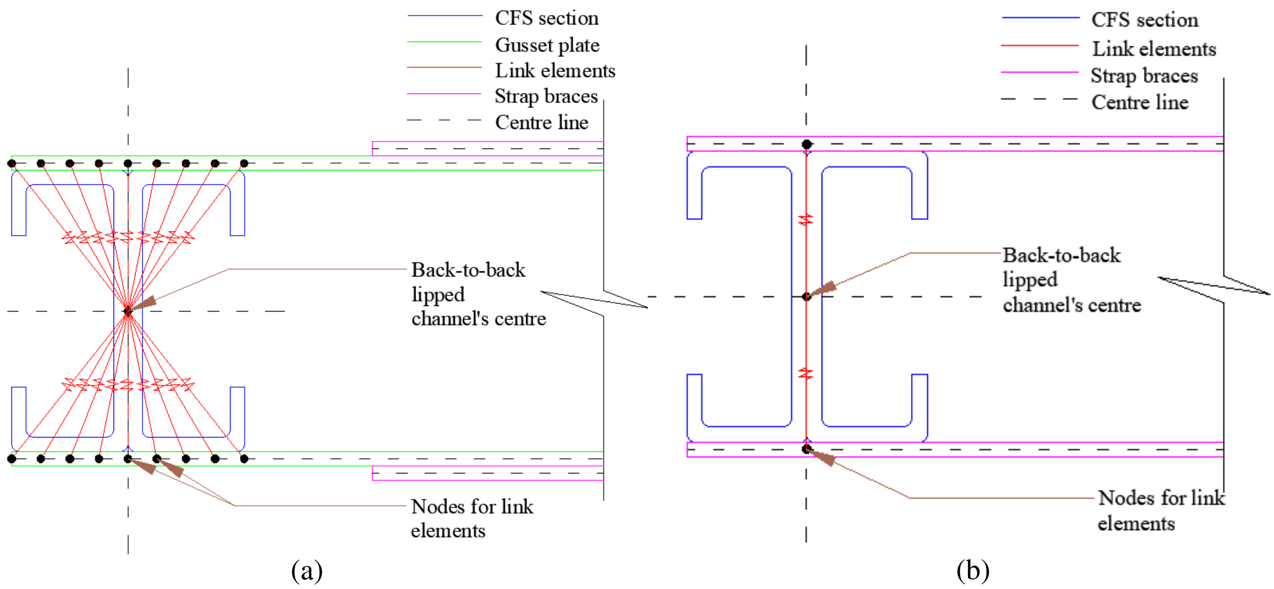

Figure 3 Cross-sectional illustration of the two-joint link connectivity of (a) strap braces, (b) gusset plates to the chord-track joints

3 DEVELOPMENT OF THE ROCKING SHEAR CONNECTION

A rocking shear wall generally has the capabilities of self-entering, provided it can rock as a rigid unit, possessing sufficient shear strength and connections that are adequate to rock. In a performance-based design, the abilities of a shear wall can form a basis of design where a particular member can be designed to deform and keep the other structural members from failing under the earthquake load. A CFS strap braced stud walls tend to uplift in the presence of lateral load with the vertical load. The first rocking structure was constructed in Wellington in 2007 in New Zealand, where the self-centring cables were attached to springs at the bottom. The earthquake inertia forces were increased by the springs when the uplift occurred and reduced the frame displacements by increasing the secant stiffness (Macrae & Clifton, 2013).

A procedure is developed to generate the shear uplift at the bottom left corner right chord track joint without allowing interaction with the other structural members. The system consists of a backing plate connected to the webs of the back-to-back CFS chords, which will help stiffen the channel's web, as shown in Figure 3. A CHS C250 L0 with an outside diameter (OD) of 33.7 mm and an inside diameter (ID) of 25.7 mm will be fillet welded to the outer surface of the plate. A grade 8.8 solid bar or AISI 4140 bar will be placed inside the CHS section. A grade 8.8 solid bar or AISI 4140 bar of yield strength, f_y, 700 MPa and ultimate strength, f_u, 860 MPa is available in diameters of 20 mm. The solid bar of 20 mm will provide a clearance of 0.7 mm.

The Young's Modulus of Elasticity for the steel section, E, is 200×10^3 MPa and the Second Moment of Area of CHS C250 L0, I, is $0.0419 \times 10^6\ mm^4$. Since the CFS wall system is a fixed sway system that is

Table 1 Description of the developed numerical models in SAP2000

List	Model number	CFS wall panel	Description
1	Model A		CFS wall panel without strap braces
2	Model B		Strap braces are connected to the chords only on one side of the wall
3	Model C		Strap braces are connected to the chords on both sides of the wall
4	Model D		Strap braces are connected to the chords only on one side of the wall through gusset plates
5	Model E	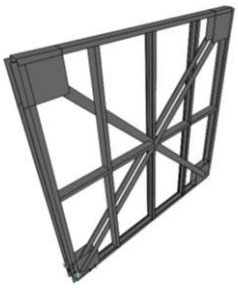	Strap braces are connected to the chords on both sides of the wall through gusset plates

fixed at each end and can sway, the translational stiffness is given by,

$$k_T = {}^{3EI}/_{L^3} \tag{1}$$

The half gap for the thickness of the CHS C250 L0 of 4 mm, and with a clearance of 0.7 mm, is 4.35 mm. Therefore, the translational stiffness, k_T turns out to be 305420 kN/mm. A 5% of the translational stiffness is adopted for the vertical stiffness, and hence the vertical stiffness, k_V, is calculated to be 15271 kN/mm. Since the chords are back-to-back double channel sections, an allowance of rotational flexibility is provided for the translational and vertical stiffnesses. As a result, the final translational and vertical stiffness, k_T and k_V is halved to 1571 kN/mm and 78.5 kN/mm, respectively.

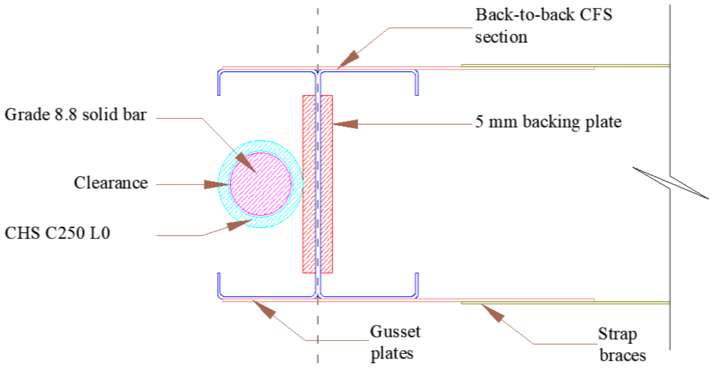

Figure 4 Proposed chord-track connection to the foundation for the tension shear uplift

Two procedures are implemented to analyse the rocking shear connection of the CFS walls in SAP2000. The *hook link property* is assigned to the X-axis, and the *gap link property* to the Z-axis to the bottom left-hand chord-track joint in the first procedure, as shown in Figure 4(a). Whereas in the second procedure, *joint spring* is assigned in the X- axis and Z-axis of the bottom left and right-hand chord-track joint, as shown in Figure 4(b). When gap and hook property is assigned to both bottom chord-track joints, the models result in instability errors, but when assigned to only the bottom left-hand chord-track joint resembled a good shear outcome. Due to the project's time constraints, the errors could not be investigated further. On the other hand, when joint springs are assigned to both bottom chord-track joints, it is observed that deformations occur at the joints. In reality, the vertical compression stiffness will be much higher than the vertical tension stiffness which is observed in the left-hand chord-track joint. In this regard, a very stiff load path on the compression side is required to obtain good overall behaviour of the CFS wall panel under shear uplift.

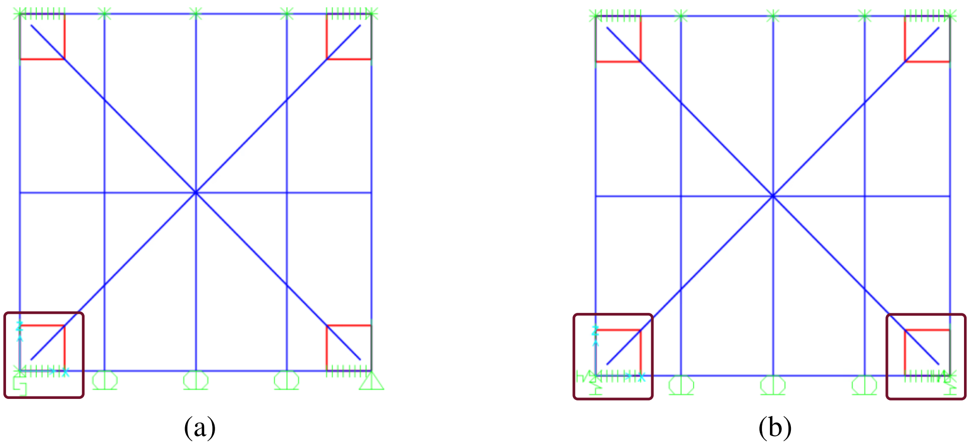

Figure 5 Model E assigned with (a) hook and gap link property at the bottom left-hand chord-track joint and (b) joint springs at both bottom left and right chord-track joint

4 ANALYSIS RESULTS AND DISCUSSIONS

In the present numerical models, the strap braces of the CFS walls are assigned a compression limit of zero, a *nonlinear property* defined in SAP2000. Therefore, nonlinear analysis is performed where two sets of load cases are assigned to the models: (a) a lateral load of 50 kN is assigned along the X-axis to simulate the lateral demand, and (b) a set of vertical loads to observe the performance of the CFS strap braced walls supporting vertical loading from the structure above and the lateral loading of 50 kN. The vertical concentrated permanent loads of 10 kN are assigned to the chord-top track and stud-top track joints representing the realistic scenario of the multi-storey building's weight being transferred from the upper-level wall panels and floors to the bottom wall panel.

According to the NZS 1170.5, the inelastic inter-storey deflection shall not exceed 2.5% for the ultimate limit state. If a ductility factor of 2 is used, then the elastic drift limit should be approximately 1.25%. The inter-storey drift ratio (IDR) of *Model A* resulted in unrealistically high lateral deflection since there is no lateral system resisting the lateral loads. The inter-storey deflection and the IDR for the five numerical models are listed in Table 2. In *Model B*, it is observed that there is an increase of 1.56% in lateral deflection from lateral load alone to lateral deflection from the combination of lateral and vertical load. Whereas in *Model D*, the increase is 4.34%, but the IDR obtained is lesser than *Model B*. For *Model C*, the percentage change is 2.36% of lateral deflection from lateral load alone to that from a combination of lateral and vertical load. *Model E,* resulted in lower inter-storey deflection than other models. The percentage change of lateral load to the combination of lateral and vertical load is 1.85%. The change in IDR is 0.45 to 0.46.

Table 2 Inter-storey drift ratio of the numerical models

Model	**Inter-storey deflection (mm)**		**Inter-storey drift (%)**	
	Lateral load	**Lateral + Vertical load**	**Lateral load**	**Lateral + Vertical load**
Model A	6731	6731	>>2.5	>>2.5
Model B	25.6	26	1.06	1.08
Model C	12.7	13	0.53	0.54
Model D	23	24	0.96	1.00
Model E	10.8	11	0.45	0.46

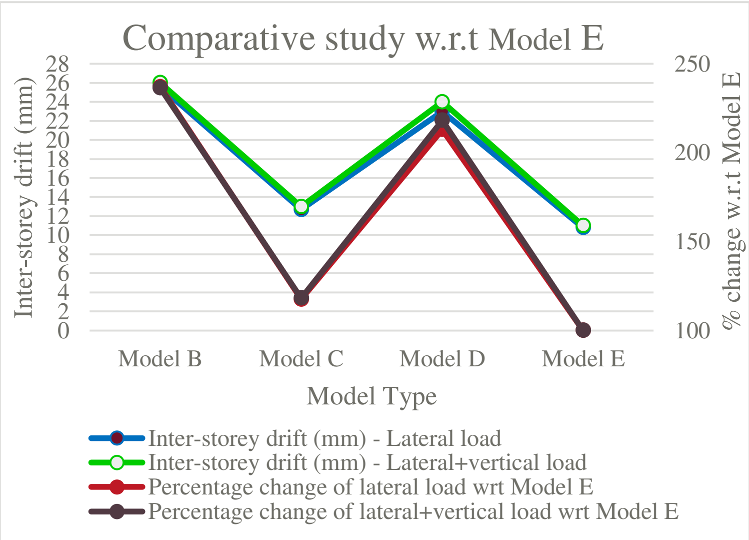

Figure 6 A comparative study on inter-storey deflection of other numerical models with respect to Model E

The IDR of all the numerical models showed acceptable limits according to NZS 1170.5. The most realistic results for straps on both sides are observed from *Model E,* and hence a comparative study is conducted to observe the response of the numerical models towards the inter-storey deflection, as shown in Figure 5. When *Model E* is compared to *Model B*, the lateral deflection in terms of lateral load and combination of the lateral and vertical load is about 2.4%, whereas the IDR decreased by 15.1% compared to *Model C*. The response changes significantly when the strap braces are connected to the chord-track connection through gusset plates. The change between *Model B* and *Model D* to *Model E* is about 10%. The lateral deflection of *Model D* is about 2.2 times that of *Model E*. The lateral deflection of *Model C* is 1.2 times that of *Model E*, which shows that the gusset plates help in resisting the lateral load and enhance the lateral performance. The comparison between *Model D* and *Model E* shows that the inter-storey deflection of *Model D* is 2 times more than *Model E* under only the lateral load and 2.2 times more than *Model E* under the combination of lateral and vertical load. The results indicate that *Model E* is more resilient towards the lateral and combination of the lateral and vertical load than *Model D*. On the other hand, the results from *Model D* demonstrates that it has the potential to resist lower-intensity earthquake load, which makes it a suitable possibility to be used in regions with lower seismic activities in the country. It also has the potential to deform elastically up to around 1% inter-storey drift, which in practice corresponds to around the maximum inter-storey drift demand observed in well-behaving structures during the very severe 22 February 2011 Christchurch earthquake (Clifton et al., 2011).

Since the section of studs are open-lipped C sections, they resulted in a slight twisting behaviour when applying lateral and a combination of the lateral and vertical loads. The twisting behaviour did not change the overall response of the wall panel; however, it increased the elastic flexibility, which could be beneficial in practice. The connection of the nogs to the studs prevented the studs from twisting or moving sideways and helped keep the wall panel stable under the lateral and vertical load application. The behaviour of the nogs indicated that the member provided rigidity and increased the studs' strength and stiffness by reducing the studs' unrestrained length by half. A lateral drift is generated in the studs due to the wall witnessing an in-plane lateral deflection when the nogs are connected to the studs through partial fixity.

The chord members of the CFS strap braced walls are back-to-back lipped C sections, and the bottom and top tracks are single-lipped C sections. The lips of the tracks are cut out to accommodate the studs and chords passing through, which makes the chords stronger than the top and bottom tracks, leading to potential track failure. A way to prevent this is to connect the chord-track-gusset plate of the wall above to that below via a translationally rigid connection in the global X direction. This type of connection will allow the horizontal component of the tension strap brace forces to get transferred into the bottom track of the wall and eventually into the top track of the bottom wall. When the lateral load of 50 kN is applied to the top left chord-track joint, the left chord results experiencing tension, whereas the right chord experiences compression. The compression results from the vertical component of the tension strap braces. When a vertical load is applied to the chords representing the multi-storey vertical load on the bottom wall, from mechanics, both the chords are in compression. The observed load paths are shown in Figure 6.

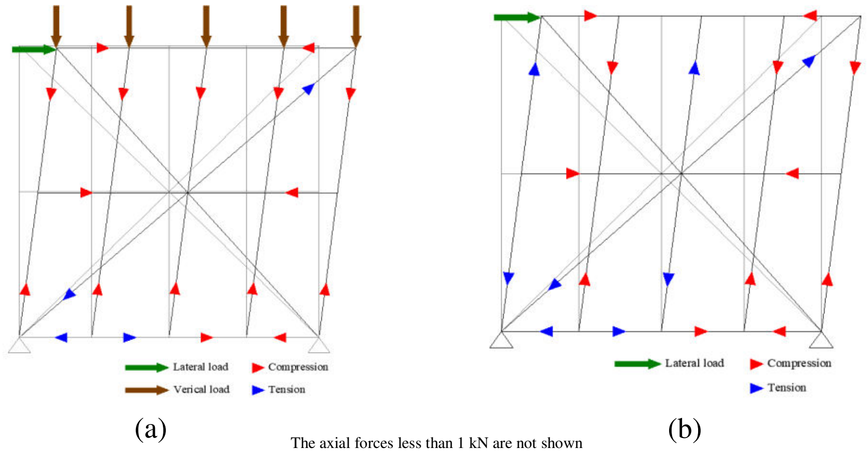

Figure 7 Load paths generated from lateral and combination of lateral and vertical load

During the static nonlinear analyses, the gusset plates showed slight divergence from the chords and tracks in *Model D*. A certain imbalance due to asymmetry was also observed in *Model B* and *Model D*. Since the gusset plates were connected to the chords and studs through a series of two joint links with six degrees of freedom, a certain amount of rotation resulted in the stud, chord flanges and edges of gusset plates. In practice, minimal divergence and rotation will be observed where the gusset plates are connected to the studs through screws on one side of the CFS wall.

When the bottom left-hand chord-track joint is assigned with hook and gap link properties, the technique predicted a good outcome for the left-hand chord-track joint. With the stiffness of 1571 kN/mm in the X axis, the deformation led to about 0.02 mm, whereas with a vertical stiffness of 78.5 N/mm, the uplift deflection is about 3 mm for *Model E*. An idea is obtained through the analysis that the vertical compression stiffness obtained in the bottom right-hand chord-track joint will be higher than the vertical tension stiffness on the left-hand chord-track joint. The result indicates that obtaining good overall performance of the CFS strap braced walls under tension uplift requires a very stiff load path on the compression side.

The inter-storey deflections and the frame actions of the numerical models – *Model B, Model C, Model D* and *Model E* are consistent with the responses observed in the study's first phase, which was conducted at the Structures Testing Laboratory at the University of Auckland. The experimental investigation was successfully ended in December 2022, and the results are currently being reported.

5 CONCLUSIONS

The present numerical study in SAP2000 considers Australasian steel, which is higher in grade and thinner in gauge in an SFRS system, to demonstrate the effects of a shear wall in the presence of lateral and vertical load. CFS strap braces are utilised as tension members to dissipate the induced energy from an earthquake load through yielding. The process is a capacity-based design, and the resulting drifts were compared to the drift limits specified in NZS 1170.5. The results obtained from the inter-storey drift ratio and frame actions depict that CFS strap-braced walls with strap braces on one side have the potential to resist lower-intensity earthquake loads, and strap braces on both sides can resist higher-intensity loads. The differences in performance in the elastic and the inelastic range are consistent with those from experimental testing, which was undertaken slightly later than this research and is soon to be released. These studies determine the utilisation of CFS strap-braced walls for mid-rise buildings in New Zealand, which will potentially increase the height of a CFS building from low-rise to mid-rise sector

6 ACKNOWLEDGEMENTS

The current study is a part of an experimental parallel research project carried out on a purpose-built test rig that can deliver a constant vertical and cyclic lateral load. The experimental investigation has been completed at the Structures Testing Lab of the University of Auckland, Newmarket, Auckland. The author would like to thank the contribution of Pouya Lotfi Rad, a PhD candidate at the University of Auckland who carried out the experimental investigation, and for sharing some of his knowledge on the application of the CFS strap braced walls.

7 REFERENCES

AISI S400. (2020). *North American Standard for Seismic Design of Cold-Formed Steel Structural Systems* (2020th ed.). American Iron and Steel Institute.

Al-Kharat, M., & Rogers, C. A. (2007). Inelastic performance of cold-formed steel strap braced walls. *Journal of Constructional Steel Research*, *63*(4), 460–474. https://doi.org/10.1016/j.jcsr.2006.06.040

AS/NZS 4600. (2018). *Cold-formed steel structures*. www.standards.govt.nz.

Clifton, C., Bruneau, M., Macrae, G., Leon, R., & Fussell, A. (2011). Steel structures damage from the Christchurch earthquake series of 2010 and 2011. *Bulletin of the New Zealand Society for Earthquake Engineering*, *44*(4).

Computer & Structures. (2022). *SAP2000* (No. v22). Computer and Structures, Inc.

Davani, M. R., Hatami, S., & Zare, A. (2016). Performance-based evaluation of strap-braced cold-formed steel frames using incremental dynamic analysis. *Steel and Composite Structures*, *21*(6), 1369–1388. https://doi.org/10.12989/scs.2016.21.6.1369

Fiorino, L., Terracciano, M. T., & Landolfo, R. (2016). Experimental investigation of seismic behaviour of low dissipative CFS strap-braced stud walls. *Journal of Constructional Steel Research*, *127*, 92–107. https://doi.org/10.1016/j.jcsr.2016.07.027

Gerami, M., & Lotfi, M. (2014). Analytical analysis of seismic behavior of cold-formed steel frames with strap brace and sheathings plates. *Advances in Civil Engineering*, *2014*. https://doi.org/10.1155/2014/535120

Hancock, G. J., & Rogers, C. A. (1998). Design of Cold-Formed Steel Structures of High Strength Steel. *Journal of Constructional Steel Research*, *46*, 1–3.

Hatami, S., Ronagh, H. R., & Azhari, M. (2008). *Behavior of thin-strap-braced cold-formed steel frames under cyclic loads*. 363–3470. https://www.researchgate.net/publication/43507396

Iuorio, O., Macillo, V., Terracciano, M. T., Pali, T., Fiorino, L., & Landolfo, R. (2014). Seismic response of Cfs strap-braced stud walls: Experimental investigation. *Thin-Walled Structures*, *85*, 466–480. https://doi.org/10.1016/j.tws.2014.09.008

Karmakar, A. (2022). *Numerical Investigation of Thin Gauge, High Strength Cold-Formed Steel Strap Braced Walls Under Combined Lateral and Vertical Loading*. The University of Auckland.

Kasaeian, S., Usefi, N., Ronagh, H., & Dareshiry, S. (2020). Seismic performance of CFS strap-braced walls using capacity-based design approach. *Journal of Constructional Steel Research*, *174*. https://doi.org/10.1016/j.jcsr.2020.106317

Lee, Y. H., Tan, C. S., Mohammad, S., Md Tahir, M., & Shek, P. N. (2014). Review on cold-formed steel connections. *The Scientific World Journal*, *2014*. https://doi.org/10.1155/2014/951216

Macillo, V., Iuorio, O., Terracciano, M. T., Fiorino, L., & Landolfo, R. (2014). Seismic response of Cfs strap-braced stud walls: Theoretical study. *Thin-Walled Structures*, *85*, 301–312. https://doi.org/10.1016/j.tws.2014.09.006

Macrae, G., & Clifton, C. (2013). *Rocking Structure Design Considerations*.

Madsen, R. L., Castle, T. A., & Schafer, B. W. (2016). *Seismic Design of Cold-Formed Steel Lateral Load-Resisting Systems: A Guide for Practicing Engineers*. *12*. https://nvlpubs.nist.gov/nistpubs/gcr/2016/NIST.GCR.16-917-38.pdf

Pourabdollah, O., Farahbod, F., & Rofooei, F. R. (2017). The seismic performance of K-braced cold-formed steel shear panels with improved connections. *Journal of Constructional Steel Research*, *135*, 56–68. https://doi.org/10.1016/j.jcsr.2017.04.008

Schafer, B. W., Ayhan, D., Leng, J., Liu, P., Padilla-Llano, D., Peterman, K. D., Stehman, M., Buonopane, S. G., Eatherton, M., Madsen, R., Manley, B., Moen, C. D., Nakata, N., Rogers, C., & Yu, C. (2016). Seismic Response and Engineering of Cold-formed Steel Framed Buildings. *Structures*, *8*, 197–212. https://doi.org/10.1016/j.istruc.2016.05.009

Standards Australia. (2021). *AS 1397:2021* (Seventh). Standards Australia.

Standards New Zealand. (2004). *Structural design actions. Part 5, Earthquake actions : New Zealand.* Standards New Zealand.

Usefi, N., Sharafi, P., & Ronagh, H. (2019). Numerical models for lateral behaviour analysis of cold-formed steel framed walls: State of the art, evaluation and challenges. *Thin-Walled Structures*, *138*(January), 252–285. https://doi.org/10.1016/j.tws.2019.02.019

Zeynalian, M., & Ronagh, H. R. (2012). A numerical study on seismic performance of strap-braced cold-formed steel shear walls. *Thin-Walled Structures*, *60*, 229–238. https://doi.org/10.1016/j.tws.2012.05.012